Thermal image encryption obtained with a SiO_2 space-variant subwavelength grating supporting surface phonon-polaritons

Nir Dahan, Avi Niv, Gabriel Biener, Vladimir Kleiner, and Erez Hasman

Optical Engineering Laboratory, Faculty of Mechanical Engineering, Technion–Israel Institute of Technology, Haifa 32000, Israel

Received June 21, 2005; revised manuscript received August 9, 2005; accepted August 9, 2005

Space-variant partially polarized thermal emission is investigated. We show that by coupling surface phonon-polaritons to a propagating field, large anisotropy of the emissivity is obtained within a narrow spectral range. We experimentally demonstrate this effect by fabricating a space-variant subwavelength grating on a SiO_2 substrate to encrypt an image in the polarization state of a thermal radiation field. © 2005 Optical Society of America

OCIS codes: 240.5420, 260.5430, 050.2770, 110.6820.

Surface phonon-polaritons (SPPs) are attributed to the coupling of an electromagnetic field with phonons at the interface of two homogeneous media. This resonant phenomenon typically occurs in the infrared region of the spectrum and involves only TM radiation. The wavenumber of SPPs is larger than that of a free-space propagating wave at the same frequency, and thus SPPs are nonradiative. Investigation of SPPs in the far field was performed by coupling the SPPs' evanescent field to a propagating field, using a prism or a grating coupler.[1,2] In one instance, by fabricating a uniform grating on a SiC substrate, a thermal source with a narrow angular peak was demonstrated.[3] With the same substrate, changing the grating parameters made it possible to produce an omnidirectional enhanced emission for a given frequency.[4] Both of these anomalous emissions were attributed to the excitation of SPPs. Recently, we demonstrated spatial manipulation of the polarization state of thermal radiation by controlling the local orientation of a fused silica (SiO_2) grating.[5,6]

In this Letter we utilize SPPs to encrypt an image in the polarization state of infrared thermal radiation. Polarization state manipulation of the thermal emission was achieved by etching a space-variant subwavelength grating on a SiO_2 substrate. The grating acted as a space-variant coupler between the propagating waves and the SPPs. Decryption of the image was obtained by measuring the polarization state of the thermal radiation and applying the correct key. Polarization encryption provides additional flexibility to conventional phase- and amplitude-based encryption methods. This feature is advantageous as it makes the optical encryption more secure.[7–9] Furthermore, unlike other polarization-based encryption schemes, ours is a passive one in that it does not require a light source. To the best of our knowledge, this is the first time that optical encryption based on thermal emission supporting SPPs has been achieved.

Consider a sample at a uniform and constant temperature. The emitted radiation from the sample is proportional to its emissivity, which is polarization dependent. Our goal is to maximize the degree of polarization (DOP) of the thermal emission within a narrow spectral band and to exploit it for polarization encryption of a thermal image. For this purpose we utilize the ability of SPPs to enhance the TM radiation using a space-variant subwavelength grating. The TM polarization state has an electric field component that is perpendicular to the grating strips. We designed an element composed of separate zones, each consisting of a subwavelength grating on a SiO_2 substrate. This material supports SPPs in the vicinity of a 9 μm wavelength, as the real part of its dielectric constant, ϵ', is smaller than -1, as shown in the inset of Fig. 1(a).[10] Consequently, a thermal image with a high discrimination of the polarization state is achieved. In this case, the emissivity of the subwavelength grating determines both the polarization state and the DOP of the thermal emission. First, we optimized a uniform SiO_2 grating by using the spectral reflectivity from a rigorous coupled wave analysis calculation to achieve the maximal emissivity modulation (EMD). EMD is defined as $\eta=|(\epsilon_{TM}-\epsilon_{TE})/(\epsilon_{TM}+\epsilon_{TE})|$, where ϵ_{TM} and ϵ_{TE} are the emissivity values of the grating for the TM and TE polarization states, respectively. The emissivity, ϵ, is related to the reflectivity, R, by Kirchhoff's law, $\epsilon=1-R$, for each direction, wavelength, temperature, and polarization. Figure 1(a) shows the calculated spectral EMD of the grating at a normal direction. An EMD resonance peak of $\eta=0.52$ is observed at an 8.93 μm wavelength. This resonance is maintained at the same wavelength for broad emission directions up to 30°, as seen in Fig. 1(b). We ascribe this phenomenon to the excitation of SPPs in the region where the dispersion curve is flat.[4] We optimized the grating for a wavelength of 8.93 μm at the normal emission direction. Figure 1(c) shows the calculated EMD as a function of the grating depth. A strong variation in the EMD is observed, with the greatest value obtained at a grating depth of $h=0.7$ μm. For this grating depth, the optimal fill factor was found to be $q=0.5$, as shown in Fig. 1(d).

To confirm our theoretical predictions, we formed a 10 mm $\times$ 10 mm uniform grating of a 2 μm period on an amorphous SiO_2 substrate using an advanced photolithographic process.[6] The inset in Fig. 2 shows

0146-9592/05/233195-3/$15.00

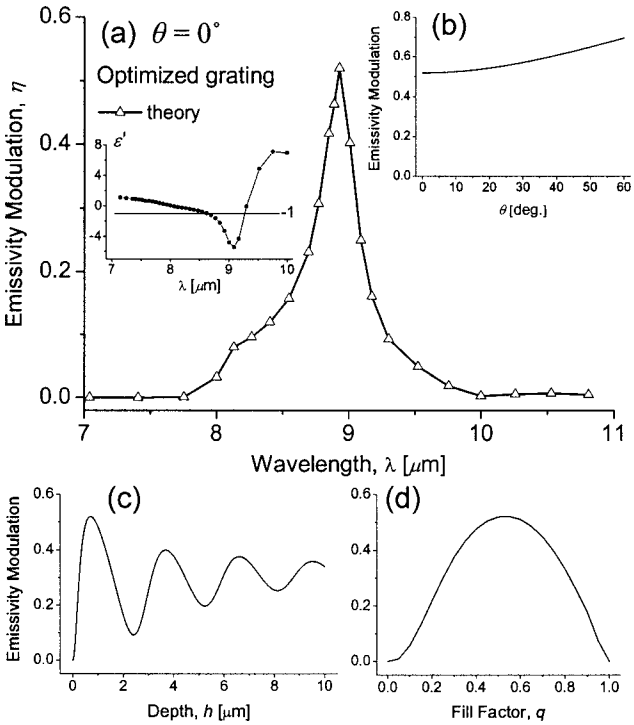

Fig. 1. (a) Calculated SiO_2 spectral EMD in the normal direction for a grating with period $\Lambda = 2$ μm, fill factor $q = 0.5$, and depth $h = 0.7$ μm. The inset shows the spectral dependence of the real part of the SiO_2 dielectric constant, ϵ'. (b) Calculated EMD as a function of the observation angle, θ, with the same parameters as in (a). (c) Calculated EMD versus grating depth for a wavelength of 8.93 μm with normal observation; grating parameters: period $\Lambda = 2$ μm, fill factor $q = 0.5$. (d) Calculated EMD versus grating fill factor (q) for a wavelength 8.93 μm with a normal direction of light; grating parameters: period $\Lambda = 2$ μm, depth $= 0.7$ μm.

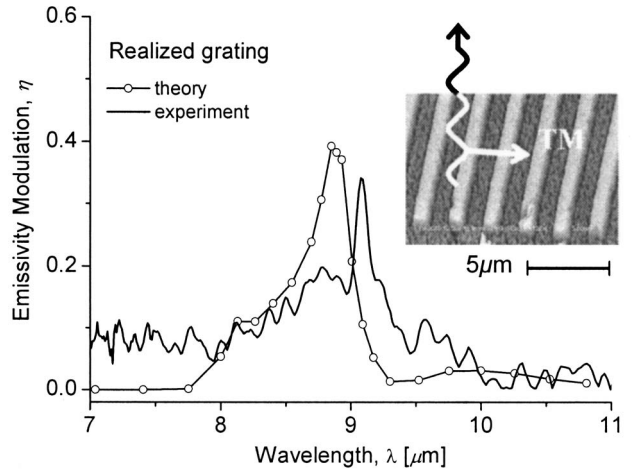

Fig. 2. Calculated (circles) and measured (solid curves) SiO_2 spectral EMD in normal direction for a grating with period $\Lambda = 2$ μm, fill factor $q = 0.3$, and depth $h = 0.8$ μm. The inset shows a SEM image of the grating.

a scanning electron microscope (SEM) image of the grating. Due to inaccuracies in fabrication, the actual fill factor was measured to be 0.3 instead of 0.5. Correspondingly, for this fill factor the optimal depth was determined to be 0.8 μm instead of 0.7 μm. For these grating parameters a peak in the EMD of $\eta = 0.38$ was calculated instead of 0.52, as can be seen in Fig. 2. The spectral measurements of thermal radiation for TM and TE polarizations were performed by using an infrared Fourier-transform spectrometer (FTIR, SP-Oriel, resolution 4 cm^{-1}) equipped with a cooled HgCdTe detector. In this experiment, the sample was heated to 873 K with a precision of better than 1 K (heater and temperature controller from HeatWave Labs Inc.). The measured EMD as a function of wavelength, at a normal emission direction, is shown in Fig. 2. A narrow spectral peak is observed at approximately the 9.07 μm wavelength. The measured EMD was $\eta = 0.33$, indicating a good agreement with our prediction. This significant EMD is expected up to an observation angle of 30°.[6] As can be seen, the measured EMD peak is redshifted with respect to the predicted value. This behavior is attributed to the temperature dependence of the dielectric constant of SiO_2.[4] Up until this point we have demonstrated a high discrimination between the TM and TE polarized emissions within a narrow spectral band. Therefore the polarization state of the thermal radiation can be modified by controlling the local orientation of the subwavelength grating.

We propose a thermal image that results from a two-dimensional array of pixels, each consisting of a uniform grating with a different orientation. In our approach, a gray-scale image function, G, is linearly related to an orientation function according to $\phi(x,y) = aG(x,y)$, where a is a constant and $0 \leqslant \phi < \pi$. Encryption is obtained by adding a scrambling key function, $\phi_k(x,y)$, to the orientation function of an encoded image, $\phi_i(x,y)$. The orientation of the actual fabricated grating is described as $\phi_e(x,y)_{\mathrm{mod}\,\pi} = \phi_i(x,y) + \phi_k(x,y)$. To decrypt the image, we need to measure the local polarization state of the field that radiates from the element. It is easy to express the space-variant polarization state of a radiation field using the Stokes vector $\mathbf{S} = (S_0, S_1, S_2, S_3)^{\mathrm{T}}$, where S_0 denotes the intensity and S_1, S_2, and S_3 describe the polarization state of the radiated light. Since the TM and TE polarization states of the thermal radiation are not correlated, we can write the emitted radiation Stokes vector as $\mathbf{S} = \mathbf{S}_{\mathrm{TM}} + \mathbf{S}_{\mathrm{TE}}$, where $\mathbf{S}_{\mathrm{TM}} = I_{\mathrm{TM}}(1, \cos 2\phi_e, -\sin 2\phi_e, 0)^{\mathrm{T}}$ and $\mathbf{S}_{\mathrm{TE}} = I_{\mathrm{TE}}(1, -\cos 2\phi_e, \sin 2\phi_e, 0)^{\mathrm{T}}$ are, respectively, the Stokes vectors of the TM and TE polarized radiations,[11] and I_{TM} and I_{TE} represent the corresponding radiated intensities. Note that this radiation is partially linearly polarized everywhere. Since only the local orientation of the linear polarization is of interest, the three Stokes parameters S_0, S_1, S_2 are sufficient. These three Stokes parameters can be obtained by imaging the element through a linear polarizer oriented at three different angles. These measurements are denoted by I_0, I_{45}, and I_{90} for a polarizer oriented at 0°, 45°, and 90°, respectively. The Stokes parameters related to these measured intensities are given by $S_0 = I_0 + I_{90}$, $S_1 = I_0 - I_{90}$, and $S_2 = 2I_{45} - S_0$. We note that the DOP (defined by $\sqrt{S_1^2 + S_2^2 + S_3^2}/S_0$) in the case of noncorrelated TM and TE polarized emissions is

given by DOP$=(I_{TM}-I_{TE})/(I_{TM}+I_{TE})$ and is equal to the EMD, η. The linear polarization state orientation of the emitted field at each pixel can be found from $\tan(2\phi_e)=-S_2/S_1$.[11] For an unauthorized receiver, ϕ_e is meaningless; however, by applying the correct key function, we can retrieve the orientation function of the primary image $\phi_i(x,y)=\phi_e(x,y)-\phi_k(x,y)$, from which the gray-scale of the original image can be reconstructed.

To implement this concept we used the photolithographic process mentioned earlier[6] to form an element to encrypt the image shown in Fig. 3(a). The key for the encrypting function used is shown in the gray-scale picture in Fig. 3(b). The element was etched on a SiO_2 substrate comprising 20×20 pixels, each with dimensions of 500 μm$\times$500 μm, with a local subwavelength grating period of 2 μm. The fabrication resulted in an actual fill factor of $q=0.45$, which produced the maximal EMD at an etching depth of $h=0.75$ μm.

A SEM image of a part of the element is shown in Fig. 3(c). Zones with different grating orientations are clearly observed. Following the fabrication stage, the encrypted element was heated to 353 K to improve the signal-to-noise ratio. A thermal camera

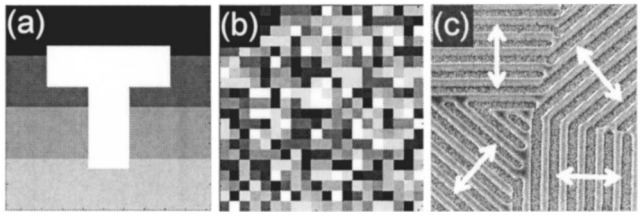

Fig. 3. (a) Gray-scale intensity of the primary image to be encrypted. (b) Orientation function of the key, ϕ_k, is shown in gray scale. (c) A SEM image of the encrypted element taken from a small region in the element. The arrows indicate the TM polarization orientation of the thermal emission near the grating.

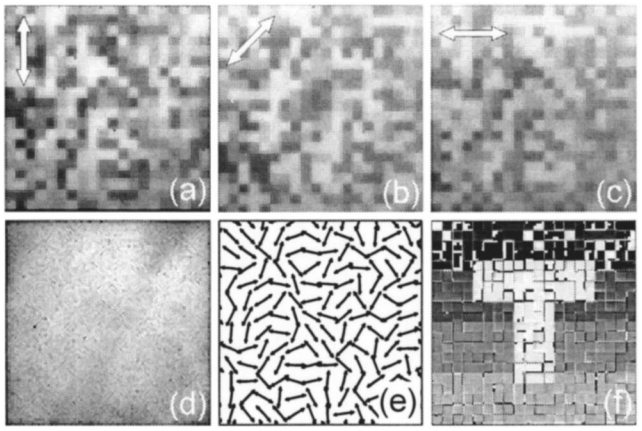

Fig. 4. Measured intensities, I_0, I_{45}, I_{90}, obtained with a polarizer in varying orientations: (a) 0°, (b) 45°, and (c) 90°. The white arrows indicate the orientation angle of the polarizer. (d) Measured intensity emitted by the encrypted element without a polarizer. (e) Measured polarization state of the emitted light from the central region of the encrypted element. (f) Decrypted image achieved by the decryption process using intensities I_0, I_{45}, I_{90}, and the correct key function, ϕ_k, shown in Fig. 3(b).

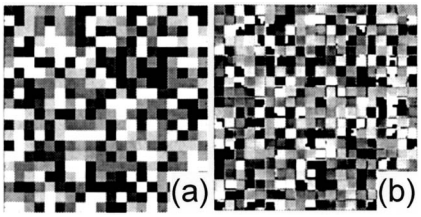

Fig. 5. (a) Orientation function of the wrong key is shown in gray scale. (b) Unsuccessfully decrypted image produced by the decryption process using intensities I_0, I_{45}, and I_{90}, but with the wrong key function.

(CEDIP, 320×240 pixels) was used to capture the emitted radiation. The thermal radiation obtained without a polarizer is shown in Fig. 4(d). In this image, the intensity distribution is uniform and decryption is therefore impossible. However, when the element is imaged through a polarizer, intensity patterns are obtained. The experimental patterns I_0, I_{45}, and I_{90} for a polarizer oriented at 0°, 45°, and 90° are shown in Figs. 4(a)–4(c), respectively. Figure 4(e) shows the various polarization state orientations that were observed experimentally. As can be seen, the polarization state is scrambled and the primary image cannot be retrieved. However, by using the correct key function [Fig. 3(b)] within the image processing, the image can be decrypted as shown in Fig. 4(f). A gray-scale pattern of a wrong key function is shown in Fig. 5(a). When this key is used the primary image is not reconstructed, as can be seen in Fig. 5(b).

In conclusion, we have demonstrated a passive optical encryption method based on thermal radiation with space-variant polarization distribution. Control of the polarization state orientation was achieved by selectively coupling the SPPs. Decryption was carried out by measuring the space-variant polarization state of the thermal radiation and applying the correct digital key function.

E. Hasman's e-mail address is mehasman@tx.technion.ac.il.

References

1. H. Raether, *Surface Plasmons on Smooth and Rough Surfaces and on Gratings* (Springer, 1988).
2. K. Joulain, J.-P. Mulet, F. Marquier, R. Carminati, and J.-J. Greffet, Surf. Sci. Rep. **57**, 59 (2005).
3. J.-J. Greffet, R. Carminati, K. Joulain, J.-P. Mulet, S. Mainguy, and Y. Chen, Nature **416**, 61 (2002).
4. F. Marquier, K. Joulain, J.-P. Mulet, R. Carminati, J.-J. Greffet, and Y. Chen, Phys. Rev. B **69**, 155412 (2004).
5. E. Hasman, G. Biener, A. Niv, and V. Kleiner, in *Progress in Optics, Vol. 47*, E. Wolf, ed. (North-Holland, 2005), pp. 215–289.
6. N. Dahan, A. Niv, G. Biener, V. Kleiner, and E. Hasman, Appl. Phys. Lett. **86**, 191102 (2005).
7. G. Biener, A. Niv, V. Kleiner, and E. Hasman, Opt. Lett. **30**, 1096 (2005).
8. O. Matoba and B. Javidi, Appl. Opt. **43**, 2915 (2004).
9. P. C. Mogensen and J. Glückstad, Opt. Commun. **173**, 177 (2000).
10. E. D. Palik, ed., *Handbook of Optical Constants of Solids* (Academic, 1985).
11. E. Collett, *Polarized Light* (Dekker, 1993).